



Image-matching digital macro-slide—a novel pathological examination method for microvascular invasion detection in hepatocellular carcinoma

Hong-Ming Yu¹ · Kang Wang¹ · Jin-Kai Feng¹ · Lei Lu² · Yu-Chen Qin³ · Yu-Qiang Cheng¹ · Wei-Xing Guo¹ · Jie Shi¹ · Wen-Ming Cong⁴ · Wan Yee Lau^{1,5} · Hui Dong⁴ · Shu-Qun Cheng¹

Received: 22 October 2021 / Accepted: 28 January 2022 / Published online: 16 March 2022

© The Author(s) 2022

Abstract

Background Microvascular invasion (MVI) is a prominent risk factor of postoperative recurrence for hepatocellular carcinoma (HCC). The MVI detection rate of conventional pathological examination approaches is relatively low and unsatisfactory.

Methods By integrating pathological macro-slide with whole-mount slide imaging, we first created a novel pathological examination method called image-matching digital macro-slide (IDS). Surgical samples from eligible patients were collected to make IDS. The MVI detection rates, tumor recurrence rates and recurrence-free survival were compared among conventional 3-Point and 7-Point baseline sampling protocols and IDS. Additionally, biomarkers to recognize MVI false negative patients were probed via combining conventional pathological sampling protocols and IDS. Receiver operating characteristic curve (ROC) analysis was used to obtain the optimal cutoff of biomarkers to distinguish MVI false negative patients.

Results The MVI detection rates were 21.98%, 32.97% and 63.74%, respectively, in 3-Point, 7-Point baseline sampling protocols and IDS ($p < 0.001$). Tumor recurrence rate of patients with MVI negative status in IDS (6.06%) was relatively lower than that of patients with MVI negative status in 3-Point (16.90%) and 7-Point (16.39%) sampling protocols. Alpha-fetoprotein (AFP) and protein induced by vitamin K absence or antagonist-II (PIVKA-II) were selected as potential biomarkers to distinguish MVI false negative patients.

Conclusions Our study demonstrated that IDS can help enhance the detection rate of MVI in HCC and refine the prediction of HCC prognosis. Alpha-fetoprotein is identified as a suitable and robust biomarker to recognize MVI false-negative patients in conventional pathological protocols.

Keywords Hepatocellular carcinoma · Microvascular invasion · 3-Point baseline sampling protocol · 7-Point baseline sampling protocol · Imaging-matching digital macro-slide · Recurrence-free survival · Receiver operating characteristic curve · AFP · PIVKA-II

Hong-Ming Yu, Kang Wang, Jin-Kai Feng and Lei Lu have contributed equally to this work.

✉ Hui Dong
huidongwh@126.com

✉ Shu-Qun Cheng
chengshuqun@aliyun.com

¹ Department of Hepatic Surgery VI, Eastern Hepatobiliary Surgery Hospital, Second Military Medical University, 225 Changhai Road, Shanghai 200433, China

² Clinical Research Center, Changhai Hospital, Second Military Medical University, 168 Changhai Road, Shanghai 200433, China

³ Department of Health Statistics, Second Military Medical University, 800 XiangYin Road, Shanghai 200433, China

⁴ Department of Pathology, Eastern Hepatobiliary Surgery Hospital, Second Military Medical University, 225 Changhai Road, Shanghai 200433, China

⁵ Faculty of Medicine, The Chinese University of Hong Kong, Shatin, Hong Kong SAR, China

Introduction

Hepatocellular carcinoma (HCC) is the fourth leading cause of cancer-related mortality worldwide and the leading cause of death among patients with cirrhosis [1]. HCC is characterized by an aggressive clinical course and dismal outcomes, with about two-thirds of patients diagnosed at advanced stage at first presentation. Up to 70–80% of HCC patients will develop disease recurrence within five years following initial curative treatments [1].

Microvascular invasion (MVI) refers to the presence of tumor cell clusters in a vascular lumen lined by endothelial cells under microscopic examination [2, 3]. It has been repeatedly demonstrated to be a prominent risk factor of postoperative recurrence for HCC patient [4, 5]. It is well known that pathological examination is the gold standard to diagnose and grade cancers via observing the morphological character, differentiation degree and growth pattern of tumor cells. Besides, pathological examination can detect some important biological factors around tumor tissues, including micro-satellites and MVI. Nevertheless, due to the limited scope of routine glass slides and randomness and bias of sampling, conventional pathological testing protocol has a tendency to under-report the incidence of MVI in HCC. Hence, constructing a novel pathological technique with greater MVI detection power is required.

Recently, based upon development of histological slide digitization and computational image processing, whole-mount slides imaging (WSI) has been popularized in oncology studies. WSI refers to scanning a complete microscope slide, capturing many small high-resolution image tiles or strips and then montaging them to create a full image of a histopathological section. Many studies have highlighted the clinical significance of WSI in assisting pathologists investigating the whole spectrum of tumor biopsy specimens, and in identifying prognostic markers and histological subtypes of various cancers [6–8]. Macroscopic histological slide (macro-slide), different from routine small slides, expands to cover the whole section of tumor tissues and maintains the integrity of tumor specimens to the greatest extent. Macro-slide has the advantage to exhibit more pathological features compared with conventional small slides.

In this study, by combining macro-slide and WSI technique, we create and first report the clinical utility of a novel pathological examination method called “image-matching digital macro-slide (IDS)” for MVI detection in HCC. We show that IDS has the capacity to remarkably increase MVI detection rates in HCC, guiding postoperative adjuvant therapies and surveillance protocols, thus reducing long-term recurrence rates. By analyzing IDS, we are able to get deeper insight into the comprehensive and most relevant features of tumors.

Methods and materials

Patients

Consecutive patients who underwent radical hepatectomy of liver cancer at Eastern Hepatobiliary Surgery Hospital (EHBH) from October 2018 to December 2019 were enrolled. The follow-up date was censored on January 31, 2021. The inclusion criteria were as follows: (I) patients aged from 20 to 70 years old, (II) Child–Pugh class A–B7, (III) Eastern Cooperative Oncology Group (ECOG) performance score was 0–1, and (IV) underwent radical resection and had complete postoperative histopathological tissues. The exclusion criteria were as follows: (I) palliative-intend resection, (II) presence of extrahepatic metastasis or major vascular invasion, (III) underwent preoperative anti-cancer treatment, (IV) a history of other malignant tumors, and (V) pathologically confirmed intrahepatic cholangiocarcinoma (ICC) or combined HCC–ICC. The study was approved by institutional review board of our hospital. Written informed consent was obtained from patients for their data to be used for research purposes.

Pathological diagnosis standard

Two experienced pathologists identified HCC and MVI in all cases, and a third pathologist participated in the identification and gave the final result when there was ambiguity. HCC was diagnosed upon the Guidelines for the Diagnosis and Treatment of Hepatocellular Carcinoma (2019 Edition) [9]. MVI was defined as a cancer cell cluster composed of ≥ 50 cells in a microscopic vessel adjacent to the primary tumor [10, 11].

Materials

The following materials were required in this study: (I) pathological sampling console, paraffin embedding station (Leica Biosystems Richmond, Inc., USA), paraffin slicing machine, cooler, dehydrator, slice drying machine, and high-resolution slice scanner; (II) Tissue embedding box (7.7 cm \times 4.3 cm \times 1.3 cm), custom-made anti-off slide glass (7.5 cm \times 5.0 cm), and custom-made cover glass (6.0 cm \times 5.0 cm); (III) special paraffin embedding mold (Leica Biosystems Richmond, Inc., USA), large paraffin block holder, and special cutter head; (IV) Olympus Automatic Digital Pathology Scanner (VS120). The customized items or equipment were shown in Fig. S1.

Intraoperative marking

When intraoperative exploration, we determined the surgical resection range and marked the cutting edge and direction. It was recommended that the cross-section of the human body be taken as the sampling plane, marked with two asymmetric directions, and photographed for filing. Consequently, it was more convenient to distinguish the direction of the tumor specimen in vitro.

Specimen processing

We determined the section according to the maximum diameter of the tumor, half of which were taken according to the 3-Point and 7-Point baseline sampling protocols (Fig. 1a; Fig. 1b), the other half of which were taken using the IDS method (Fig. 1c). After the specimen was detached, 10% neutral formaldehyde should be injected as soon as possible (within 30 min) and fixed continuously for not less than 48 h. According to the direction of sampling and section, the thickness of the specimen was 0.5–1.0 cm, and the maximum size of the trimmed specimen was 6.0 cm × 5.0 cm. If the specimen was too large, it could be divided into several parts as required.

Grossing and paraffin embedding

The specimens were rinsed for formaldehyde with water for at least 2 h. Tissue automatic dehydrator was used to dehydrate specimens, which were then dried using slice drying machine. Next, the specimens were put into and soaked the liquid paraffin. The tissue specimens were embedded and shaped using paraffin embedding station and special paraffin embedding mold. The required sections were confirmed and adjusted again when shaping the tissues.

Serial sectioning and Hematoxylin–Eosin (HE) staining

When serial sectioning, the paraffin block was fixed with large holder. Paraffin slicing machine and matched special cutter head for big paraffin block were used to make sections with a thickness of 3 μm. After fished out, the slides were baked at 75 °C for 15 min with a baking machine, so that

the tissues and the slides can be firmly adhered. The sections were stained with hematoxylin and eosin for histological examination.

Digital scanning and analysis

All tissue sections were scanned with a high-resolution slice scanner and corresponding image data were stored. The images were analyzed using the software matched with the scanner for parameters such as micro-metastases, stromal cell proportion, peripheral inflammatory changes, etc. The image data were matched with the scanned images, and the characteristics of pathological and imaging changes were analyzed again. Digital image signals in the region could be analyzed according to the research content.

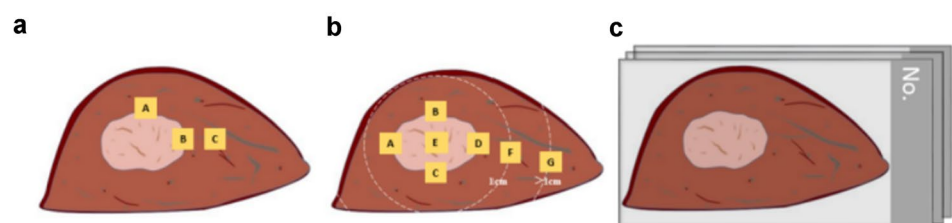
Follow-up

Patients were followed up with laboratory tests including tumor biomarkers and liver biochemistry, abdominal ultrasonography, and contrast-enhanced CT once every 3–6 months. The diagnosis of intrahepatic recurrence was made by imaging findings alone if the tumor displayed typical enhancement characteristics; otherwise, the recurrent diseases were biopsied. Recurrence-free survival (RFS) time was calculated from the date of first surgery to the date when there was a clear evidence of recurrent disease.

Statistical analysis

Continuous variables were expressed as mean (standard deviation) or median (interquartile range) and compared using student's *t* test or Mann–Whitney *U* test according to the distribution of variables. Categorical variables were compared using chi-square test or Fisher's exact test. Survival curves were generated using the Kaplan–Meier method and compared using the log-rank test. Receiver operating characteristic curve (ROC) analysis was used to obtain the optimal cutoff value of AFP and PIVKA-II to distinguish MVI false negative patients. Clinical performance of 3-Point, 7-Point and IDS to identify MVI actual positive was assessed by the sensitivity, specificity, and predictive values. Statistical analyses were performed by SPSS 26.0 software

Fig. 1 The model of different pathological sampling methods: **a** 3-Point baseline sampling protocol. **b** 7-Point baseline sampling protocol. **c** IDS sampling protocol



(SPSS, Inc., Chicago, IL, USA) and R 3.6.3 software (R Development Core Team). *p* values less than 0.05 indicated statistical significance.

Results

The detailed process of IDS

Preoperative MRI showed that the tumor was located in the posterior lower segment of the right lobe of the liver. The size of the tumor was 72 mm × 58 mm × 55 mm. T2W1 showed slightly higher, equal, and uneven equal-high signals. Scanning after enhancement, the hepatic artery phase demonstrated obvious uneven enhancement. In the portal phase and delayed phase, the relative signal attenuation was in line with the primary liver cancer (Fig. 2a). The preoperative evaluation was in accordance with the inclusion criteria. During the operation, the tumor was completely resected (R0 resection), and the whole specimen was taken to produce macro-slide. After hematoxylin–eosin staining, the macro-slide was observed at different positions with various magnifications (Fig. 2b). Then, the pathological macro-slide was matched with tumor specimen and imaging data to obtain WSI including MVI positions (Fig. 2c). This total process was named as IDS. The detailed preparation and production process of IDS is shown in the flow diagram (Fig. S2). Another two representative HCC cases with histopathological details focused on MVI are shown in Fig. S3.

The baseline characteristics and long-term outcomes of eligible patients

A total of 110 primary liver cancer patients were collected in this study. 19 patients who were pathologically diagnosed as intrahepatic cholangiocarcinoma were excluded, and 91 HCC patients were finally included. Using surgically resected specimens from 91 HCC patients, 145 thick slices were produced and examined. Conventional pathology covers tumor in all three extents. In this study, 300 sections in 3-Point, 664 sections in 7-Point, and 145 sections in IDS were examined and compared.

The baseline clinicopathological characteristics are shown in Table 1. Almost all patients had hepatitis B or C virus infection background. The percentage of hepatitis B virus infection was 96.7%, and only one patient did not have hepatitis. The liver function of patients was all graded as Child–Pugh class A. The median tumor size was 3.80 cm. In 4 HCC patients associated with portal vein tumor thrombus (PVTT), PVTT existed in the branches of main portal vein and could be resected

radically. The shortest and longest follow-up times were 13 and 28 months, respectively. 24 (26.37%) patients developed disease recurrence and 5 patients (5.49%) died during follow-up.

MVI detection rates in 3-Point, 7-Point baseline sampling protocols and IDS

As shown in Fig. 3a, the detection rates of MVI were 21.98%, 32.97% and 63.74%, respectively, in 3-Point, 7-Point and IDS ($p < 0.001$). Patients with MVI positive status in 3-Point and 7-Point were all included in MVI positive status in IDS. The populations of 3-Point and 7-Point were not exactly the same (Fig. 3b). Among patients with MVI negative status in 3-Point and 7-Point, the two populations were partly different, but they all included MVI negative status in IDS (Fig. 3c). Therefore, in this study, the specificity and sensitivity of IDS on MVI detection were both 100%, while the specificity of 3-Point and 7-Point on MVI detection were both 100%, and the sensitivity of 3-Point and 7-Point on MVI detection were only 34% and 52%, respectively (Table 2). The above results showed that IDS had superior sensitivity and specificity for the detection of MVI than 3-Point and 7-Point.

Tumor recurrence rates in three various pathological examination methods

To compare the impact of MVI, which was detected by 3-Point, 7-Point and IDS, respectively, on tumor recurrence, survival analyses were performed (Fig. 4a–c). Under the three methods, patients with MVI positive status were more likely to relapse ($p < 0.001$, $p < 0.001$, $p = 0.001$, respectively). We found that 12 (16.90%) HCC patients with MVI negative status in 3-Point had tumor recurrence, and 2 patients died due to disease progression. In 7-Point sampling method, 10 (16.39%) patients with MVI negative status had recurrence (relapse time range: 2.1–14.4 months), including 2 recurrence-related deaths. In IDS, 2 (6.06%) patients with MVI negative status recurred (relapse time: 13.13 and 14.40 months), and no deaths occurred. Next, we did subgroup analysis combining IDS with 3-Point and 7-Point. Results showed that patients with MVI positive status in both 3-Point and IDS, and in both 7-Point and IDS were most prone to recur. Patients with MVI positive status in IDS were more likely to relapse than patients with actual MVI negative status ($p = 0.021$, $p = 0.016$). (Fig. 4d–e). It is to say, 3-Point and 7-Point sampling protocols have a potential possibility to miss MVI, and patients with MVI false negative status in 3-Point and 7-Point are more likely to recur than patients with actual MVI negative status in all three MVI pathological testing methods.

Fig. 2 A case of image-matching digital macro-slide. **a** Preoperative MRI and sample selection of the patient: 1, T1WI; 2, T2WI; 3, DWI; 4, arterial phase; 5, portal phase; 6, delayed phase. **b** image after WSI scanning: 1, making macro-slide samples; 2, the overall view of the image after the sample is scanned and stitched; 3, mixed nodular cirrhosis was observed after magnification of 20 times; 4, local hemorrhagic necrosis was seen inside the tumor after magnification of 100 times; 5, MVI was observed after magnification of 200 times; 6, accumulation of inflammatory cells in the tumor was observed after 400-fold magnification. **c** corresponding specimen and digital macro-slide combined to MRI imaging (T2WI): 1, specimen; 2, digital macro-slide; 3, MRI imaging (T2WI), in 1: 1. Marking the different vessels and MVI locations with different colors in the panel

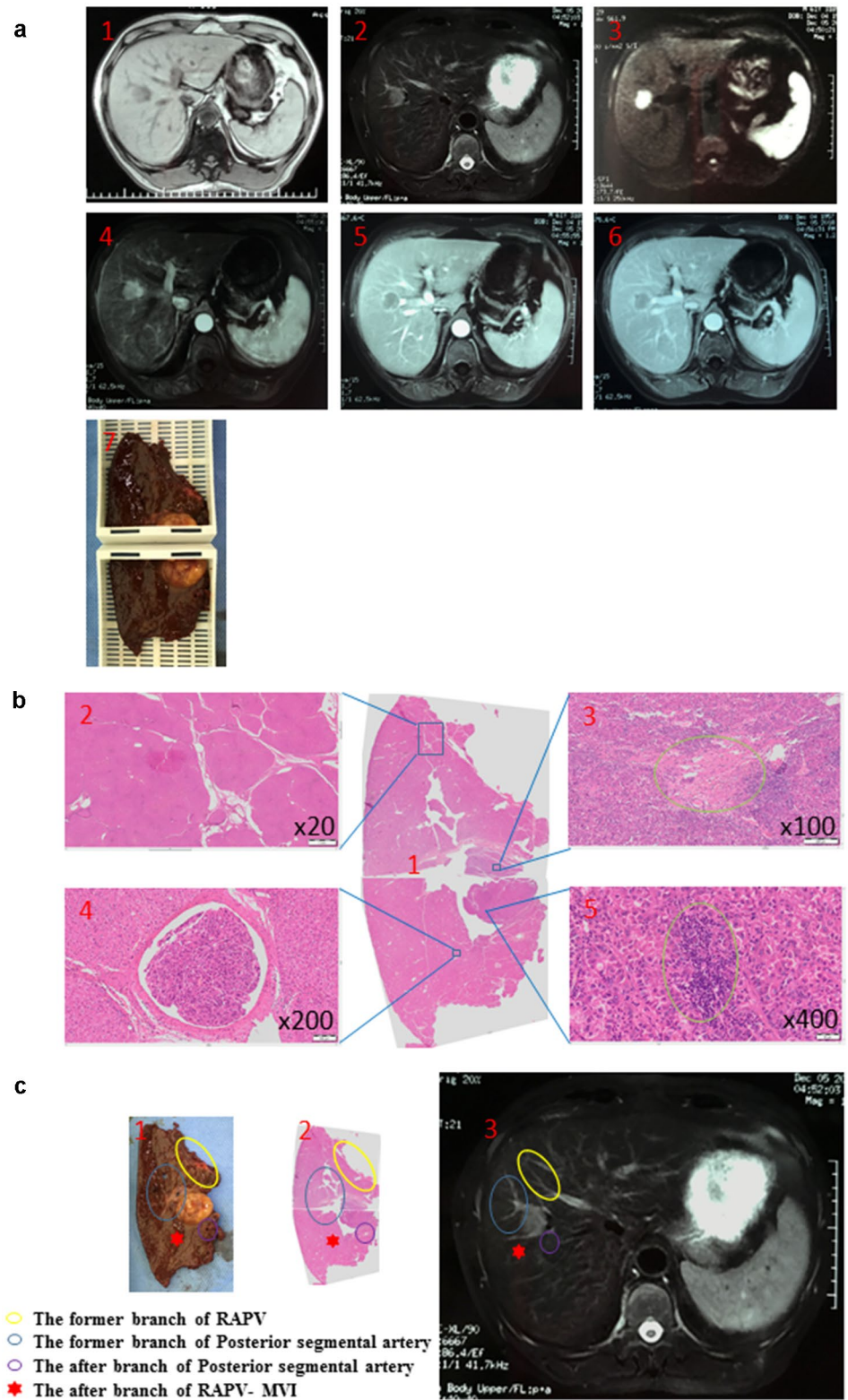


Table 1 Baseline characteristics of patients with hepatocellular carcinoma

Variables	Total (n=91)
Gender, n (%)	
Female	13 (14.29)
Male	78 (85.71)
Age (year), Mean ± SD	56.58 ± 9.30
HBsAg, n (%)	
Negative	14 (15.38)
Positive	77 (84.62)
HBeAg, n (%)	
Negative	74 (81.32)
Positive	17 (18.68)
HBcAb, n (%)	
Negative	3 (3.30)
Positive	88 (96.70)
HBV-DNA, n (%)	
< 1000 copies/mL	53 (58.24)
≥ 1000 copies/mL	38 (41.76)
HCV, n (%)	
Negative	87 (95.60)
Positive	4 (4.40)
AFP, Median (Q1, Q3), ug/L	26.70 (5.45, 511.25)
PIVKA-II, Median (Q1, Q3), mAU/mL	274.00 (62.50, 1172.00)
CA199, Median (Q1, Q3), U/mL	15.50 (8.65, 28.60)
CEA, Median (Q1, Q3), ug/L	2.60 (1.70, 3.40)
ALT, Median (Q1, Q3), U/L	25.00 (16.00, 44.00)
AST, Median (Q1, Q3), U/L	25.00 (18.00, 38.00)
Total bilirubin, Median (Q1, Q3), umol/L	14.30 (10.85, 18.10)
GGT, Median (Q1, Q3), U/L	39.00 (25.00, 77.00)
Albumin, Mean ± SD, g/L	42.90 ± 4.45
GLU, Median (Q1, Q3), mmol/L	5.12 (4.79, 5.65)
ALP, Median (Q1, Q3), U/L	77.00 (59.50, 98.00)
WBC, Median (Q1, Q3), 10 ⁹ /L	4.81 (3.73, 5.72)
RBC, Mean ± SD, 10 ¹² /L	4.57 ± 0.47
HGB, Mean ± SD, g/L	140.80 ± 15.47
PLT, Mean ± SD, 10 ⁹ /L	149.08 ± 61.11
PT, Median (Q1, Q3), s	11.50 (11.00, 12.05)
Tumor size, Median (Q1, Q3), cm	3.80 (2.50, 5.50)
Tumor number, n (%)	
1	83 (91.21)
2	7 (7.69)
4	1 (1.10)
PVTT, n (%)	
Absence	87 (95.60)
Presence	4 (4.40)
Encapsulation, n (%)	
No	23 (25.27)
Incomplete	42 (46.15)
Complete	26 (28.57)
Liver cirrhosis, n (%)	
No	38 (41.76)

Table 1 (continued)

Variables	Total (n=91)
Yes	53 (58.24)
Child–Pugh class A, n (%)	91 (100.00)
Recurrence, n (%)	
No	67 (73.62)
Yes	24 (26.37)

HBsAg hepatitis B surface antigen, *HBeAg* hepatitis B e antigen, *HBcAb* hepatitis B core antibody, *HBV-DNA* hepatitis B virus-deoxyribonucleic acid, *HCV* hepatitis C virus, *AFP* alpha-fetoprotein, *PIVKA-II* protein induced by vitamin K antagonist-II, *CA199* carbohydrate antigen199, *CEA* carcinoembryonic antigen, *ALT* alanine aminotransferase, *AST* aspartate aminotransferase, *GGT* γ -glutamyltransferase, *GLU* glucose, *ALP* alkaline phosphatase, *WBC* white blood cells, *RBC* red blood cells, *PLT* platelet, *PT* prothrombin time, *PVTT* portal vein tumor thrombus

Identification of potential biomarkers to distinguish MVI false negative patients in conventional pathological sampling protocols

In order to find out the clinicopathological characteristics of patients with missed MVI in 3-Point and 7-Point, IDS was matched with 3-Point and 7-Point. As shown in Table 3, there were significant differences in 3-Point in AFP, PIVKA-II, ALP, and tumor number. The medians of AFP between 3-Point negative IDS negative and 3-Point negative IDS positive groups were 6.10 (3.10, 20.30) ug/L and 81.30 (10.12, 560.65) ug/L. The medians of PIVKAI between 3-Point negative IDS negative and 3-Point negative IDS positive groups were 107.00 (33.00, 412.00) mAU/mL and 449.00 (90.50, 3168.75) mAU/mL. The medians of ALP between 3-Point negative IDS negative and 3-Point negative IDS positive groups were 79.00 (63.00, 92.00) U/L and 64.50 (54.25, 79.25) U/L. As shown in Table 4, only AFP and PIVKA-II had significant differences in 7-Point. The medians of AFP between 7-Point negative IDS negative and 7-Point negative IDS positive groups were 6.10 (3.10, 20.30) ug/L and 160.55 (20.92, 1210.00) ug/L. The medians of PIVKA-II between 7-Point negative IDS negative and 7-Point negative IDS positive groups were 107.00 (33.00, 412.00) mAU/mL and 460.50 (239.25, 3084.25) mAU/mL, respectively. It revealed that AFP and PIVKA-II could be potential biomarkers to distinguish MVI false negative patients in 3-Point and 7-Point.

Comparison of sensitivity and specificity of AFP and PIVKA-II in identifying MVI false negative patients

In order to study the sensitivity and specificity of AFP and PIVKA-II to identify MVI false negative patients, 71 patients with MVI positive and negative status in IDS but

Fig. 3 **a** MVI detection rate under 3-point baseline sampling protocol, 7-point baseline sampling protocol and image matching digital macro-slide. **b**, **c** the composition of MVI positive and negative status patients in different detective methods (3-point baseline sampling protocol, 7-point baseline sampling protocol and image matching digital macro-slide)

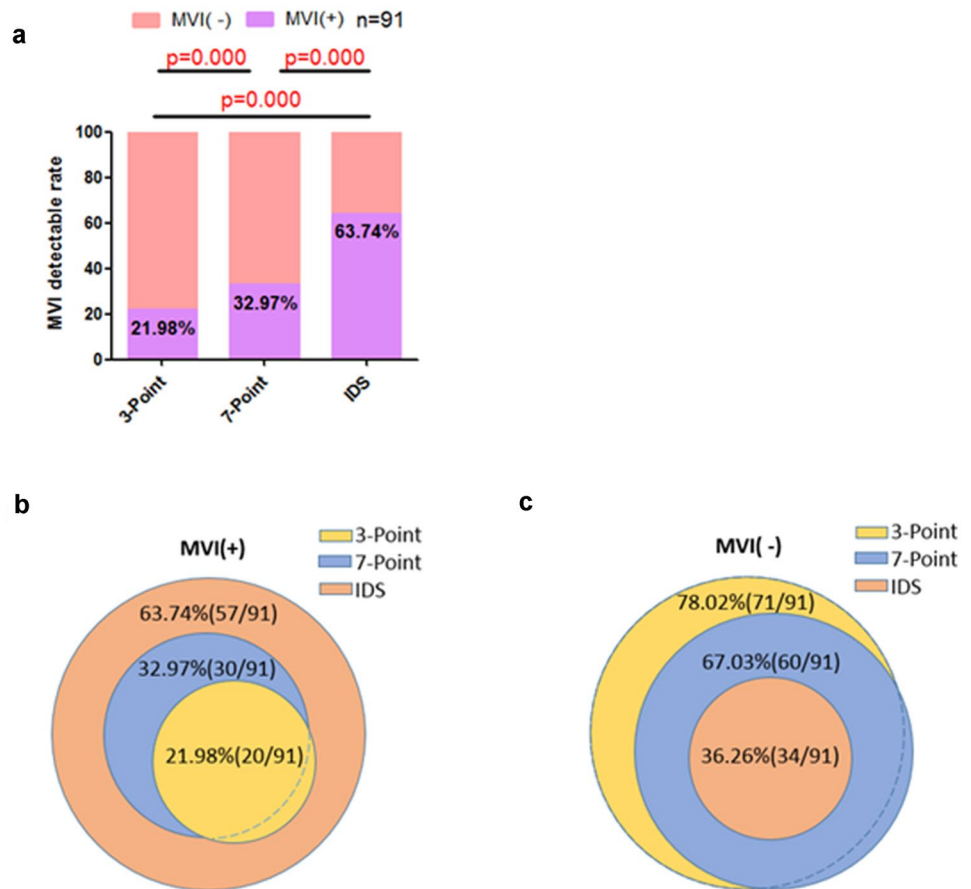


Table 2 MVI sensitivity and specificity under 3-Point, 7-Point and IDS

Metrics	3-Point	7-Point
Accuracy	0.58 (0.47–0.68)	0.69 (0.59–0.78)
Sensitivity	0.34 (0.22–0.48)	0.52 (0.38–0.65)
Specificity	1.00 (0.89–1.00)	1.00 (0.89–1.00)
Positive predictive value	1.00 (0.83–1.00)	1.00 (0.88–1.00)
Negative predictive value	0.46 (0.35–0.59)	0.54 (0.41–0.67)

MVI microvascular invasion, 3-Point 3-point baseline sampling protocol, 7-Point 7-point baseline sampling protocol, IDS image-matching digital macro-slide

both negative in 3-Point were compared, and a total of 61 patients with MVI positive and negative status in IDS but both negative in 7-Point were compared. After calculating the best cutoff by maximizing the Youden index (Table 5), in 3-Point, when AFP was divided by a cutoff of 22.5 ng/mL, the AUC was 0.715 (0.592–0.837), the sensitivity was 0.68 (0.51–0.82), and the specificity was 0.79 (0.61–0.91). When using 267 mAU/mL as the cutoff of PIVKA-II, the AUC was 0.665 (0.538–0.793), the sensitivity was 0.66 (0.49–0.80),

and the specificity was 0.67 (0.48–0.82) (Fig. 5a–b). In 7-Point, when AFP was divided by a cutoff of 23.9 ng/mL, the AUC was 0.748 (0.617–0.879), the sensitivity was 0.75 (0.55–0.89), and the specificity was 0.79 (0.61–0.91). When using 267 mAU/mL as the cutoff of PIVKA-II, the AUC was 0.696 (0.558–0.833), the sensitivity was 0.75 (0.55–0.89), and the specificity was 0.67 (0.47–0.81) (Fig. 5c–d). Therefore, AFP is superior to PIVKA-II as a biomarker to distinguish MVI false negative patients.

Potential clinical utility of upper limit of AFP normal value to identify MVI false negative patients in conventional pathological MVI sampling protocols

Because the cutoff values of AFP in 3-Point and 7-Point (22.5 and 23.9 ng/mL) were similar to the upper limit of normal value of AFP (20 ng/mL), the comparison and analysis were carried out using 22.5 ng/mL and 20 ng/mL, 23.9 ng/mL and 20 ng/mL respectively. In 3-Point sampling method, the detection rate of patients with MVI false negative status was 68.4% (26/38), and there was a significant difference (Fig. 5e, Table 6). In 7-Point sampling method (Fig. 5f,

Fig. 4 MVI related recurrence-free survival. **a** MVI detected by 3-point baseline sampling protocol and related recurrence-free survival. **b** MVI detected by 7-point baseline sampling protocol and related recurrence-free survival. **c** MVI detected by image matching digital macro-slide and related recurrence-free survival. **d** 3-point baseline sampling protocol combined with image matching digital macro-slide to detect MVI and related recurrence-free survival. **e** 7-point baseline sampling protocol combined with image matching digital macro-slide to detect MVI and related recurrence-free survival

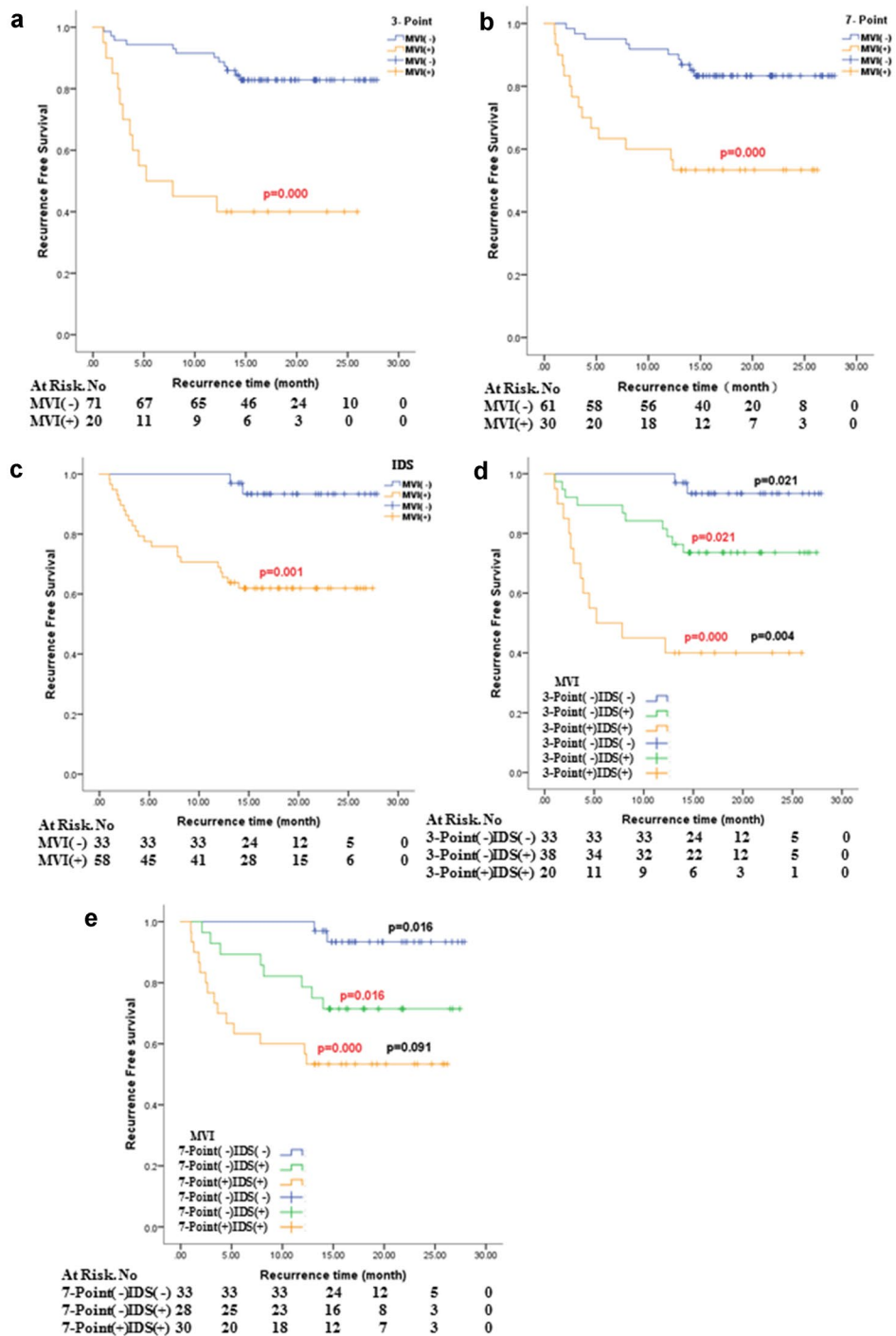


Table 7), the detection rates of patients with MVI false negative status patients were 75% (21/28) and 70% (21/30) respectively, both of which were significantly different. That is to say, in 3-Point and 7-Point, 68.4% and 70% of patients with MVI negative status and with AFP greater than 20 ng/mL are likely to be false negative.

Discussion

HCC is characterized as a complex and heterogeneous disease with diverse individual outcomes. MVI is one of the most prominent features and important prognostic factors of long-term survival in HCC. The reported detection rate

Table 3 The clinicopathological features were compared in different combinations of 3-Point and IDS with MVI or not

Variables	3-Point (-) IDS (-) (n=33)	3-Point (-) IDS (+) (n=38)	3-Point (+) IDS (+) (n=20)	p
Gender, n (%)				0.690
Female	4 (30.77)	7 (53.85)	2 (15.38)	
Male	29 (37.18)	31 (39.74)	18 (23.08)	
Age (year), Mean ± SD	57.09 ± 8.96	56.84 ± 9.50	55.25 ± 9.80	0.768
HBsAg, n (%)				0.603
Negative	7 (50.00)	5 (35.71)	2 (14.29)	
Positive	26 (33.77)	33 (42.86)	18 (23.38)	
HBeAg, n (%)				0.654
Negative	28 (37.84)	29 (39.19)	17 (22.97)	
Positive	5 (29.41)	9 (52.94)	3 (17.65)	
HBcAb, n (%)				0.603
Negative	2 (66.67)	1 (33.33)	0 (0.00)	
Positive	31 (35.23)	37 (42.05)	20 (22.73)	
HBV-DNA, n (%)				0.921
< 1000 copies/mL	20 (37.74)	22 (41.51)	11 (20.75)	
≥ 1000 copies/mL	13 (34.21)	16 (42.11)	9 (23.68)	
HCV, n (%)				0.826
Negative	31 (35.63)	37 (42.53)	19 (21.84)	
Positive	2 (50.00)	1 (25.00)	1 (25.00)	
AFP, Median (Q1, Q3), ug/L	6.10 (3.10, 20.30)	81.30 (10.12, 560.65)	346.35 (31.43, 1210.00)	<0.001
PIVKA- II, Median (Q1, Q3), mAU/mL	107.00 (33.00, 412.00)	449.00 (90.50, 3168.75)	290.50 (137.50, 866.25)	0.032
CA199, Median (Q1, Q3), U/mL	14.00 (6.60, 21.10)	17.50 (9.50, 28.52)	18.00 (9.35, 36.15)	0.263
CEA, Median (Q1, Q3), ug/L	2.80 (2.00, 3.70)	2.70 (1.90, 3.27)	1.70 (1.37, 3.23)	0.168
ALT, Median (Q1, Q3), U/L	25.00 (15.00, 50.00)	20.50 (14.25, 33.75)	27.50 (21.50, 54.25)	0.199
AST, Median (Q1, Q3), U/L	25.00 (17.00, 36.00)	21.50 (18.00, 37.50)	32.50 (23.00, 39.00)	0.222
Total bilirubin, Median (Q1, Q3), umol/L	15.30 (12.20, 18.10)	14.10 (11.57, 17.53)	14.05 (9.50, 20.38)	0.788
GGT, Median (Q1, Q3), U/L	38.00 (25.00, 71.00)	32.00 (24.00, 61.75)	52.00 (39.25, 103.00)	0.069
Albumin, Mean ± SD, g/L	43.09 ± 3.74	42.32 ± 4.65	43.71 ± 5.15	0.505
GLU, Median (Q1, Q3), mmol/L	5.24 (4.89, 6.07)	5.03 (4.67, 5.44)	5.29 (5.01, 5.95)	0.231
ALP, Median (Q1, Q3), U/L	79.00 (63.00, 92.00)	64.50 (54.25, 79.25)	89.50 (72.25, 103.50)	0.017
WBC, Median (Q1, Q3), 10 ⁹ /L	4.87 (3.97, 6.26)	4.81 (3.73, 5.64)	4.54 (3.29, 5.74)	0.587
RBC, Mean ± SD, 10 ¹² /L	4.53 ± 0.48	4.60 ± 0.42	4.60 ± 0.57	0.779
HGB, Mean ± SD, g/L	141.33 ± 14.19	140.58 ± 16.48	140.35 ± 16.25	0.969
PLT, Mean ± SD, 10 ⁹ /L	159.39 ± 71.71	149.55 ± 54.17	131.15 ± 52.85	0.267
PT, Median (Q1, Q3), s	11.50 (10.90, 11.90)	11.50 (11.00, 12.12)	11.60 (11.07, 12.15)	0.697
Tumor size, Median (Q1, Q3), cm	3.50 (2.50, 4.30)	3.65 (2.08, 6.12)	5.00 (3.50, 6.08)	0.127
Tumor number, n (%)				0.009
1	33 (39.76)	35 (42.17)	15 (18.07)	
2	0 (0.00)	3 (42.86)	4 (57.14)	
4	0 (0.00)	0 (0.00)	1 (100.00)	
PVTT, n (%)				0.203
Absence	33 (37.93)	36 (41.38)	18 (20.69)	
Presence	0 (0.00)	2 (50.00)	2 (50.00)	
Encapsulation, n (%)				0.195
No	4 (17.39)	13 (56.52)	6 (26.09)	
Incomplete	16 (38.10)	16 (38.10)	10 (23.81)	
Complete	13 (50.00)	9 (34.62)	4 (15.38)	
Liver cirrhosis, n (%)				0.624
No	13 (34.21)	18 (47.37)	7 (18.42)	
Yes	20 (37.74)	20 (37.74)	13 (24.53)	
Child–Pugh class A, n (%)	33 (36.26)	38 (41.76)	20 (21.98)	1.000

3-Point 3-point baseline sampling protocol, MVI microvascular invasion, IDS image-matching digital macro-slide, HBsAg hepatitis B surface antigen, HBeAg hepatitis B e antigen, HBcAb hepatitis B core antibody, HBV-DNA hepatitis B virus-deoxyribonucleic acid, HCV hepatitis C virus, AFP alpha-fetoprotein, PIVKA-II protein induced by vitamin K antagonist-II, CA199 carbohydrate antigen199, CEA carcinoembryonic

Table 3 (continued)

antigen, *ALT* alanine aminotransferase, *AST* aspartate aminotransferase, *GGT* γ -glutamyltransferase, *GLU* glucose, *ALP* alkaline phosphatase, *WBC* white blood cells, *RBC* red blood cells, *PLT* platelet, *PT* prothrombin time, *PVTT* portal vein tumor thrombus

of MVI in HCC was relatively low in previous studies, ranging from 15.0 to 33.8% after liver resection or transplantation [12–15]. Because of the limited range of ordinary glass slides and the varied criteria in pathological sampling protocol, the conventional pathological testing approach tends to undervalue the presence of MVI in HCC. Therefore, establishing a novel and practical pathological examination approach which can increase MVI detection rate is urgently needed.

With the breakthrough of WSI techniques, high-resolution macro-pathological digital pictures can be acquired. After combining the digital pathological macro-slide data with the imaging informational of patients, the pathological information including the distribution and characteristics of MVI can be accurately mapped to the corresponding images. This novel pathological examination technique is named as IDS. The major difference of IDS and WSI is the slide formats and sizes. IDS sufficiently takes advantage of macro-slide as its bridging vehicle of pathological and imaging information.

The present study first reported the clinical utility of IDS in detecting MVI in HCC. In this study, we showed that IDS had a higher MVI detection rate than classical pathological examination approaches. In our study, the detection rate of MVI using IDS was significantly higher than conventional pathological approaches (63.7 vs. 33.0% or 22.0%), indicating that IDS had superior power in MVI detection compared with classical method.

Additionally, we provided evidence that in patients diagnosed with MVI negative status, the recurrence rate was significantly lower using IDS compared with conventional pathological method (6.1 vs. 16.4% or 16.9%), suggesting it can guide postoperative surveillance and adjuvant treatments through screening those patients with MVI false-negative status (that is, MVI was detected by IDS but undetected by conventional pathological testing) in conventional pathological methods, thus reducing long-term recurrence rates. Furthermore, IDS and conventional pathological testing could complement with each other mutually. Our findings demonstrated that patients detected as MVI positive in both IDS and conventional pathological protocols were most likely to occur disease recurrence in the near future following initial hepatic surgery. The recurrence rate of patients with MVI

false-negative status was substantially higher than that of patients with actual MVI negative status.

We also selected AFP as a suitable and robust biomarker to identify MVI false-negative patients in conventional pathological protocol. Approximately 70% of HCC patients who were diagnosed as MVI negative status in conventional pathological examination may be MVI positive status in IDS testing. This encouraging result showed that IDS outperformed conventional pathological method in MVI detection for patients with abnormal AFP. For patients with normal AFP level (≤ 20 ng/mL) and MVI negative status in conventional pathological method, IDS was also a crucial way to confirm the actual MVI status.

Previously, Sheng et al. [16] proposed a standardized pathological proposal for evaluating MVI of HCC. They concluded that the MVI detection rate determined by seven-point sampling protocol (SPSP) was significantly higher than that determined by 3-point sampling method (47.1 vs. 34.5%, $p=0.048$). Nevertheless, there was no marked difference in MVI detection rate between SPSP and 13-point sampling method (47.1 vs. 51.3%, $p=0.517$). Therefore, we suppose that it is a futile effort to simply increase the sampling numbers beyond 7 points in conventional pathological slides. Contrarily, IDS is a useful and promising pathological technique to further increase MVI detection rates on the basis of conventional pathological testing method, thus guiding the subsequent treatment strategies of patients with MVI.

The potential application of IDS in clinical practice goes beyond MVI detection. In our on-going study, the locations of MVI can be accurately positioned using IDS, providing a reliable way to explore the distribution patterns of MVI in HCC and other tumors. Additionally, IDS can facilitate in judging the degree of tumor necrosis and observing the infiltration of inflammatory and immune cells, which can improve the efficacy evaluation of non-surgical treatments, such as transarterial chemoembolization, tyrosine kinase inhibitors and immune checkpoint inhibitors.

This study has some limitations. First, the small sample size and observational nature of this study may potentially affect the results. Second, all of the patients included in this study had a background of HBV infection. Whether IDS is applicable to patients with other etiologies of HCC needs further investigation. Third, this study is based upon our

Table 4 The clinicopathological features were compared in different combinations of 7-Point and IDS with MVI or not

Variables	7P (–) MS (–) (n=33)	7P (–) MS (+) (n=28)	7P (+) MS (+) (n=30)	p
Gender, n (%)				0.147
Female	4 (30.77)	7 (53.85)	2 (15.38)	
Male	29 (37.18)	21 (26.92)	28 (35.90)	
Age (year), Mean ± SD	57.09 ± 8.96	57.32 ± 10.30	55.33 ± 8.86	0.670
HBsAg, n (%)				0.474
Negative	7 (50.00)	4 (28.57)	3 (21.43)	
Positive	26 (33.77)	24 (31.17)	27 (35.06)	
HBeAg, n (%)				0.267
Negative	28 (37.84)	20 (27.03)	26 (35.14)	
Positive	5 (29.41)	8 (47.06)	4 (23.53)	
HBcAb, n (%)				0.641
Negative	2 (66.67)	1 (33.33)	0 (0.00)	
Positive	31 (35.23)	27 (30.68)	30 (34.09)	
HBV-DNA, n (%)				0.942
< 1000 copies/mL	20 (37.74)	16 (30.19)	17 (32.08)	
≥ 1000 copies/mL	13 (34.21)	12 (31.58)	13 (34.21)	
HCV, n (%)				0.458
Negative	31 (35.63)	26 (29.89)	30 (34.48)	
Positive	2 (50.00)	2 (50.00)	0 (0.00)	
AFP, Median (Q1, Q3), ug/L	6.10 (3.10, 20.30)	160.55 (20.92, 1210.00)	66.35 (13.67, 1210.00)	<0.001
PIVKA-II, Median (Q1, Q3), mAU/mL	107.00 (33.00, 412.00)	460.50 (239.25, 3084.25)	257.00 (90.50, 725.75)	0.021
CA199, Median (Q1, Q3), U/mL	14.00 (6.60, 21.10)	19.50 (11.17, 30.35)	15.40 (8.62, 33.60)	0.336
CEA, Median (Q1, Q3), ug/L	2.80 (2.00, 3.70)	2.70 (2.08, 3.12)	1.90 (1.33, 3.53)	0.170
ALT, Median (Q1, Q3), U/L	25.00 (15.00, 50.00)	22.50 (16.25, 36.50)	25.00 (17.25, 46.75)	0.853
AST, Median (Q1, Q3), U/L	25.00 (17.00, 36.00)	24.00 (18.00, 39.50)	26.50 (18.25, 37.75)	0.936
Total bilirubin, Median (Q1, Q3), umol/L	15.30 (12.20, 18.10)	13.55 (11.38, 17.88)	15.05 (9.85, 19.00)	0.789
GGT, Median (Q1, Q3), U/L	38.00 (25.00, 71.00)	32.00 (24.00, 63.00)	45.00 (30.50, 86.00)	0.471
Albumin, Mean ± SD, g/L	43.09 ± 3.74	41.79 ± 4.70	43.74 ± 4.84	0.242
GLU, Median (Q1, Q3), mmol/L	5.24 (4.89, 6.07)	5.21 (4.94, 5.68)	5.02 (4.75, 5.40)	0.392
ALP, Median (Q1, Q3), U/L	79.00 (63.00, 92.00)	66.50 (54.75, 83.00)	79.00 (60.75, 101.75)	0.246
WBC, Median (Q1, Q3), 10 ⁹ /L	4.87 (3.97, 6.26)	4.43 (3.43, 5.54)	5.02 (3.66, 5.64)	0.473
RBC, Mean ± SD, 10 ¹² /L	4.53 ± 0.48	4.56 ± 0.41	4.64 ± 0.52	0.611
HGB, Mean ± SD, g/L	141.33 ± 14.19	139.46 ± 15.06	141.47 ± 17.50	0.862
PLT, Mean ± SD, 10 ⁹ /L	159.39 ± 71.71	144.00 ± 57.54	142.47 ± 51.41	0.481
PT, Median (Q1, Q3), s	11.50 (10.90, 11.90)	11.55 (11.15, 12.70)	11.45 (11.00, 11.88)	0.610
Tumor size, Median (Q1, Q3), cm	3.50 (2.50, 4.30)	4.00 (2.45, 6.32)	4.65 (2.73, 6.00)	0.254
Tumor number, n (%)				0.053
1	33 (39.76)	24 (28.92)	26 (31.33)	
2	0 (0.00)	4 (57.14)	3 (42.86)	
4	0 (0.00)	0 (0.00)	1 (100.00)	
PVTT, n (%)				0.153
Absence	33 (37.93)	27 (31.03)	27 (31.03)	
Presence	0 (0.00)	1 (25.00)	3 (75.00)	
Encapsulation, n (%)				0.181
No	4 (17.39)	8 (34.78)	11 (47.83)	
Incomplete	16 (38.10)	13 (30.95)	13 (30.95)	
Complete	13 (50.00)	7 (26.92)	6 (23.08)	
Liver cirrhosis, n (%)				0.942
No	13 (34.21)	12 (31.58)	13 (34.21)	
Yes	20 (37.74)	16 (30.19)	17 (32.08)	
Child–Pugh class A, n (%)	33 (36.26)	28 (30.77)	30 (32.97)	1.000

7-Point 7-point baseline sampling protocol, MVI microvascular invasion, IDS image matching digital macro-slide, HBsAg hepatitis B surface antigen, HBeAg hepatitis B e antigen, HBcAb hepatitis B core antibody, HBV-DNA hepatitis B virus-deoxyribonucleic acid, HCV hepatitis C virus, AFP alpha-fetoprotein, PIVKA-II protein induced by vitamin K antagonist-II, CA199 carbohydrate antigen199, CEA carcinoembryonic

Table 4 (continued)

antigen, *ALT* alanine aminotransferase, *AST* aspartate aminotransferase, *GGT* γ -glutamyltransferase, *GLU* glucose, *ALP* alkaline phosphatase, *WBC* white blood cells, *RBC* red blood cells, *PLT* platelet, *PT* prothrombin time, *PVTT* portal vein tumor thrombus

Table 5 The cutoff value of AFP and PIVKA-II to detect MVI in 3-Point and 7-Point baseline sampling protocol

Metrics	3-Point		7-Point	
	AFP Optimal Cutoff ≥ 22.5 ng/mL	PIVKA-II Optimal Cutoff ≥ 267 mAU/mL	AFP Optimal Cutoff ≥ 23.9 ng/mL	PIVKA-II Optimal Cutoff ≥ 267 mAU/mL
Accuracy	0.73 (0.61–0.83)	0.66 (0.54–0.77)	0.77 (0.65–0.87)	0.70 (0.57–0.81)
Sensitivity	0.68 (0.51–0.82)	0.66 (0.49–0.80)	0.75 (0.55–0.89)	0.75 (0.55–0.89)
Specificity	0.79 (0.61–0.91)	0.67 (0.48–0.82)	0.79 (0.61–0.91)	0.67 (0.48–0.82)
Positive Predictive Value	0.79 (0.61–0.91)	0.69 (0.52–0.84)	0.75 (0.55–0.89)	0.66 (0.47–0.81)
Negative Predictive Value	0.68 (0.51–0.82)	0.63 (0.45–0.79)	0.79 (0.61–0.91)	0.76 (0.56–0.90)

AFP alpha-fetoprotein, *PIVKA-II* protein induced by vitamin K antagonist-II, *MVI* microvascular invasion, *3-Point* 3-point baseline sampling protocol, *7-Point* 7-point baseline sampling protocol

single-center data. The findings derived from this study require external validations.

Conclusions

This study demonstrates that imaging matching digital macro-slide (IDS) first implemented by our team can help improve the detection rate of MVI in HCC and refine the

prediction of HCC prognosis. It highlights the importance of establishment of a novel pathological algorithm of IDS to study HCC more comprehensively and allow for a better understanding of number and distribution of MVI under microscope. In the future, combining with artificial intelligence-driven approaches, IDS has the opportunity to be the standardized pathological examination method in all types of cancers.

Fig. 5 a, b, The ROC curve of AFP and PIVKA-II to predict MVI false negative status under 3-point baseline sampling protocol. **c, d,** The ROC curve of AFP and PIVKA-II to predict MVI false negative status under 7-point baseline sampling protocol. **e** AFP normal value and cutoff value to distinguish MVI false negative status under 3-point baseline sampling protocol. **f** AFP normal value and cutoff value to distinguish MVI false negative status under 7-point baseline sampling protocol

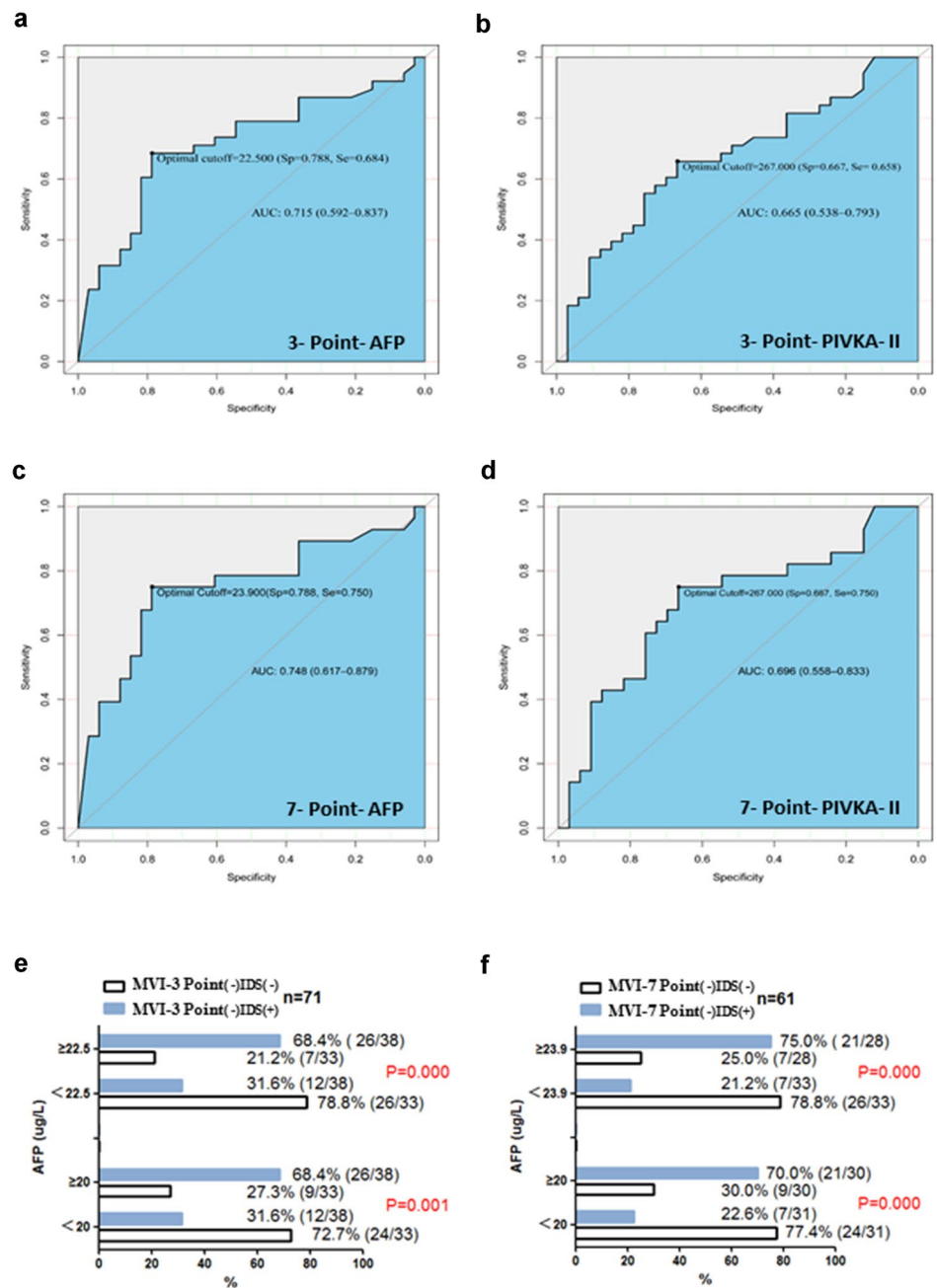


Table 6 AFP normal value and cutoff value to distinguish MVI false negative status under 3-point baseline sampling protocol

Variables	Total (n = 71)	MVI-3P (-) IDS (-) (n = 33)	MVI-3P (-) IDS (+) (n = 38)	p	Statistic
AFP, n (%)				0.001	10.375
< 20 ng/mL	36 (50.70%)	24 (66.67%)	12 (33.33%)		
≥ 20 ng/mL	35 (49.30%)	9 (25.71%)	26 (74.29%)		
AFP, n (%)				< 0.001	12.433
< 22.5 ng/mL	39 (54.93%)	26 (66.67%)	13 (33.33%)		
≥ 22.5 ng/mL	32 (45.07%)	7 (21.88%)	25 (78.12%)		

AFP alpha-fetoprotein, MVI microvascular invasion, 3P 3-point baseline sampling protocol, IDS Image-matching digital macro-slide

Table 7 AFP normal value and cutoff value to distinguish MVI false negative status under 7-point baseline sampling protocol

Variables	Total (<i>n</i> = 61)	MVI-7P (–) IDS (–) (<i>n</i> = 33)	MVI-7P (–) IDS (+) (<i>n</i> = 28)	<i>p</i>	Statistic
AFP, <i>n</i> (%)				<0.001	11.962
< 20 ng/mL	31 (50.82%)	24 (77.42%)	7 (22.58%)		
≥ 20 ng/mL	30 (49.18%)	9 (30.00%)	21 (70.00%)		
AFP, <i>n</i> (%)				<0.001	15.549
< 23.9 ng/mL	33 (54.10%)	26 (78.79%)	7 (21.21%)		
≥ 23.9 ng/mL	28 (45.90%)	7 (25.00%)	21 (75.00%)		

AFP alpha-fetoprotein, MVI microvascular invasion, 7P 7-point baseline sampling protocol, IDS Image-matching digital macro-slide

Supplementary Information The online version contains supplementary material available at <https://doi.org/10.1007/s12072-022-10307-w>.

Author contributions S-QC, HD, H-MY, KW, J-KF, LL: Conception and design. S-QC: Administrative support. Y-QC, W-XG, JS: Provision of study materials or patients. H-MY, KW, J-KF, LL, W-MC: Collection and assembly of data. H-MY, KW, J-KF, LL, WYL: Data analysis and interpretation. Y-CQ: Statistical analysis. All authors: Manuscript writing. All authors: Final approval of manuscript.

Funding The Key Project of the National Natural Science Foundation of China (No: 81730097); the Grants of the Science Fund for Creative Research Groups (No: 81521091); the National Natural Science Foundation of China (No: 81602523, 82072618); and Shanghai Municipal Health Bureau (No: SHDC2020CR1004A).

Data availability Data sets analyzed in the study can be provided by the corresponding author on reasonable request.

Declarations

Conflict of interest Hong-Ming Yu, Kang Wang, Jin-Kai Feng, Lei Lu, Yu-Chen Qin, Yu-Qiang Cheng, Wei-Xing Guo, Jie Shi, Wen-Ming Cong, Wan Yee Lau, Hui Dong, Shu-Qun Cheng have no conflicts of interest to declare.

Ethical approval This study was conducted in accordance with the Declaration of Helsinki (as revised in 2013) and approved by the Eastern Hepatobiliary Surgery Hospital (EHBH) Clinical Research Ethics Committee.

Consent to participate All patients provided informed consent for data to be used for research purposes, and no personal information was disclosed.

Open Access This article is licensed under a Creative Commons Attribution 4.0 International License, which permits use, sharing, adaptation, distribution and reproduction in any medium or format, as long as you give appropriate credit to the original author(s) and the source, provide a link to the Creative Commons licence, and indicate if changes were made. The images or other third party material in this article are included in the article's Creative Commons licence, unless indicated otherwise in a credit line to the material. If material is not included in the article's Creative Commons licence and your intended use is not permitted by statutory regulation or exceeds the permitted use, you will need to obtain permission directly from the copyright holder. To view a copy of this licence, visit <http://creativecommons.org/licenses/by/4.0/>.

References

- Llovet JM, Kelley RK, Villanueva A, Singal AG, Pikarsky E, Roayaie S, et al. Hepatocellular carcinoma. *Nat Rev Dis Primers* 2021;7(1):6
- Feng LH, Dong H, Lau WY, Yu H, Zhu YY, Zhao Y, et al. Novel microvascular invasion-based prognostic nomograms to predict survival outcomes in patients after R0 resection for hepatocellular carcinoma. *J Cancer Res Clin Oncol* 2017;143(2):293–303
- Wang H, Wu MC, Cong WM. Microvascular invasion predicts a poor prognosis of solitary hepatocellular carcinoma up to 2 cm based on propensity score matching analysis. *Hepatol Res* 2019;49(3):344–354
- Wang H, Qian YW, Wu MC, Cong WM. Liver resection is justified in patients with BCLC intermediate stage hepatocellular carcinoma without microvascular invasion. *J Gastrointest Surg* 2020;24(12):2737–2747
- Sumie S, Kuromatsu R, Okuda K, Ando E, Takata A, Fukushima N, et al. Microvascular invasion in patients with hepatocellular carcinoma and its predictable clinicopathological factors. *Ann Surg Oncol* 2008;15(5):1375–1382
- Mercan E, Mehta S, Bartlett J, Shapiro LG, Weaver DL, Elmore JG. Assessment of machine learning of breast pathology structures for automated differentiation of breast cancer and high-risk proliferative lesions. *JAMA Netw Open* 2019;2(8):e198777
- Halama N, Zoernig I, Spille A, Michel S, Kloor M, Grauling-Halama S, et al. Quantification of prognostic immune cell markers in colorectal cancer using whole slide imaging tumor maps. *Anal Quant Cytol Histol* 2010;32(6):333–340
- Wang H, Jiang Y, Li B, Cui Y, Li D, Li R. Single-cell spatial analysis of tumor and immune microenvironment on whole-slide image reveals hepatocellular carcinoma subtypes. *Cancers (Basel)* 2020;12(12):3562
- Zhou J, Sun H, Wang Z, Cong W, Wang J, Zeng M, et al. Guidelines for the diagnosis and treatment of hepatocellular carcinoma (2019 Edition). *Liver Cancer* 2020;9(6):682–720
- Cong WM, Bu H, Chen J, Dong H, Zhu YY, Feng LH, et al. Practice guidelines for the pathological diagnosis of primary liver cancer: 2015 update. *World J Gastroenterol* 2016;22(42):9279–9287
- Zhang X, Li J, Shen F, Lau WY. Significance of presence of microvascular invasion in specimens obtained after surgical treatment of hepatocellular carcinoma. *J Gastroenterol Hepatol* 2018;33(2):347–354
- Dudek K, Kornasiewicz O, Remiszewski P, Kobryń K, Ziarkiewicz-Wróblewska B, Górnicka B, et al. Impact of tumor characteristic on the outcome of liver transplantation in patients with hepatocellular carcinoma. *Transplant Proc* 2009;41(8):3135–3137
- Huang ZY, Liang BY, Xiong M, Zhan DQ, Wei S, Wang GP, et al. Long-term outcomes of repeat hepatic resection in patients with

- recurrent hepatocellular carcinoma and analysis of recurrent types and their prognosis: a single-center experience in China. *Ann Surg Oncol* 2012;19(8):2515–2525
14. Mazzaferro V, Llovet JM, Miceli R, Bhoori S, Schiavo M, Mariani L, et al. Predicting survival after liver transplantation in patients with hepatocellular carcinoma beyond the Milan criteria: a retrospective, exploratory analysis. *Lancet Oncol* 2009;10(1):35–43
 15. Fan ST, Poon RT, Yeung C, Lam CM, Lo CM, Yuen WK, et al. Outcome after partial hepatectomy for hepatocellular cancer within the Milan criteria. *Br J Surg* 2011;98(9):1292–1300
 16. Sheng X, Ji Y, Ren GP, Lu CL, Yun JP, Chen LH, et al. A standardized pathological proposal for evaluating microvascular invasion of hepatocellular carcinoma: a multicenter study by LCPGC. *Hepatol Int* 2020;14(6):1034–1047

Publisher's Note Springer Nature remains neutral with regard to jurisdictional claims in published maps and institutional affiliations.